Impact of coagulation on SARS-CoV-2 and PMMoV viral signal in wastewater solids

Nada Hegazy (nhega051@uottawa.ca)
University of Ottawa Faculty of Engineering https://orcid.org/0000-0003-4277-076X

Xin Tian
University of Ottawa Faculty of Engineering

Patrick M. D'Aoust
University of Ottawa Faculty of Engineering

Lakshmi Pisharody
University of Ottawa Faculty of Engineering

Syeda Tasneem Towhid
University of Ottawa Faculty of Engineering

Élisabeth Mercier
University of Ottawa Faculty of Engineering

Zhihao Zhang
University of Ottawa Faculty of Engineering

Shen Wan
University of Ottawa Faculty of Engineering

Ocean Thakali
University of Ottawa Faculty of Engineering

Md Pervez Kabir
University of Ottawa Faculty of Engineering

Wanting Fang
University of Ottawa Faculty of Engineering

Tram B. Nguyen
University of Ottawa Faculty of Engineering

Nathan T. Ramsay
University of Ottawa Faculty of Engineering

Alex E. MacKenzie
Children's Hospital of Eastern Ontario Research Institute

Tyson E. Graber
Children's Hospital of Eastern Ontario Research Institute

Stéphanie Guilherme
University of Ottawa Faculty of Engineering

Robert Delatolla

University of Ottawa

Research Article

Keywords: coagulation, normalization, partitioning, primary sludge, wastewater surveillance

Posted Date: July 7th, 2023

DOI: https://doi.org/10.21203/rs.3.rs-3001706/v1

Version of Record: A version of this preprint was published at Environmental Science and Pollution Research on December 19th, 2023. See the published version at https://doi.org/10.1007/s11356-023-31444-1.

Abstract

Wastewater surveillance (WWS) has received interest from researchers, scientists, and public health units for its application in monitoring active COVID-19 cases and detecting outbreaks. While WWS of SARS-CoV-2 has been widely applied worldwide, a knowledge gap exists concerning the effects of enhanced primary clarification, the application of coagulant to primary clarifiers, on SARS-CoV-2 and PMMoV quantification for reliable wastewater-based epidemiology. Ferric-based chemical coagulants are extensively used in enhanced clarification, particularly for phosphorus removal, in North America, and Europe. This study examines the effects of coagulation with ferric sulfate on the measurement of SARS-CoV-2 and PMMoV viral measurements in wastewater primary sludge and hence also settled solids. The addition of Fe^{3+} to wastewater solids ranging from 0 to 60 mg/L caused no change in N1 and N2 gene region measurements in wastewater solids, where Fe^{3+} concentrations in primary clarified sludge represent the conventional minimum and maximum concentrations of applied ferric-based coagulant. However, elevated Fe^{3+} concentrations were shown to be associated with a statistically significant increase in PMMoV viral measurements in wastewater solids, which consequently resulted in the underestimation of PMMoV normalized SARS-CoV-2 viral signal measurements (N1 and N2 copies/copies of PMMoV). pH reduction from coagulant addition did not contribute to the increase in PMMoV measurements. Thus, this phenomenon is likely attributed to the partitioning of PMMoV particles to the solids of wastewater from the bulk liquid phase of wastewater.

Highlights

- Effects of primary coagulation on SARS-CoV-2 and PMMoV measurements are unknown.
- Fe^{3+} addition to 60 mg/L had no effect on SARS-CoV-2 N1 and N2 measurements.
- Fe^{3+} addition to 60 mg/L elevated PMMoV measurements due to enhanced liquid-to-solid partitioning
- Fe^{3+} addition to 60 mg/L underrepresents PMMoV-normalized N1 and N2 measurements.
- pH change associated with Fe^{3+} addition has no effect on PMMoV-normalized N1 and N2 measurements.

1 Introduction

Wastewater surveillance (WWS) efforts for monitoring active COVID-19-positive cases are ongoing worldwide and are playing a major role in the early detection of community outbreaks (Ahmed et al., 2020; Arora et al., 2020; Bivins et al., 2020; D'Aoust et al., 2021a; Gonzalez et al., 2020; La Rosa et al., 2021; Mao et al., 2020; McClary-Gutierrez et al., 2021; Medema et al., 2020; Polo et al., 2020; Randazzo et al., 2020a, 2020b; Sims and Kasprzyk-Hordern, 2020; Thompson et al., 2020; Wu et al., 2020). Solids-based viral extraction protocols for measuring SARS-CoV-2 in wastewater have been shown to perform well with samples rich in solids such as primary sludge, raw wastewater influent, and municipal

wastewaters collected within sewered infrastructure (Balboa et al., 2020; D'Aoust et al., 2021b; Graham et al., 2021; Peccia et al., 2020; Petala et al., 2021; Westhaus et al., 2021; Wu et al., 2020). Previous studies suggest significant and/or higher sensitivity of SARS-CoV-2 RNA detection from testing primary sludge compared to testing influent (D'Aoust et al., 2021b, 2021a; Graham et al., 2021; Peccia et al., 2020; Zulli et al., 2021). Additionally, the estimation of COVID-19 disease incidence and clinical positive cases was proven to be enhanced with the normalization of the SARS-CoV-2 RNA viral signal measurements with pepper mild mottle virus (PMMoV) as a human-associated indicator that represents the fecal content of wastewater samples (D'Aoust et al., 2021b; Graham et al., 2021; Kitamura et al., 2021; Wolfe et al., 2021; Wu et al., 2021). Similar to SARS-CoV-2 RNA, PMMoV viral RNA is also consistently detected at significantly higher concentrations in the solids fraction of wastewaters (D'Aoust et al., 2021b; Jafferali et al., 2021; Kitajima et al., 2018; Rosario et al., 2009; Wu et al., 2020).

The design and operation of primary sludge treatment processes may impact the sensitivity of SARS-CoV-2 and PMMoV measurements in wastewater solids. One such design and operational consideration is the addition of chemical coagulants in enhanced primary clarification treatment. Enhanced primary sludge treatment is the process of adding coagulants to primary clarifier units (Metcalf and Eddy, 2014; Shewa and Dagnew, 2020), to enhance the removal of suspended solids and phosphorus from wastewater (Cornel and Schaum, 2009; Metcalf and Eddy, 2014; Shewa and Dagnew, 2020). In Canada, the United States, and Europe, 18.1%, 24%, and 48% of wastewater treatment plants apply primary treatment which includes chemical precipitation/flocculation (ECCC, 2011; EPA, 2022; European Environment Agency, 2022). Chemical elimination of phosphorus and suspended solids during primary clarification is commonly achieved with trivalent metal coagulants, mainly ferric-based salts (e.g. sulfate or chloride) or dissolved aluminum (alum i.e., aluminum sulfate) (Crittenden et al., 2012; Metcalf and Eddy, 2014). Ferric salts in particular are extensively used for removing phosphorus during primary clarification across North America (Crittenden et al., 2012; Davis, 2010; ECCC, 2010; Mckinnon et al., 2018; Toronto Water, 2009; U.S. EPA, 2000; Yeoman et al., 1988) and the UK (Carliell-Marquet et al., 2010). Optimal ferric sulfate dosage (usually expressed as the concentration of Fe^{3+}) in primary treatment range between 5 and 250 mg/L as Fe^{3+} depending on influent wastewater quality and treatment objectives (Crittenden et al., 2012; Pal, 2017). In conventional enhanced primary clarification systems, the optimal ferric sulfate dosage range between 5 and 60 mg/L as Fe^{3+} (Dong et al., 2019; Pal, 2017). Ferric and aluminum coagulant ions may also be ultimately to added water resource recovery facilities (WRRFs) through discharge of coagulant sludge in sewersheds from drinking water treatment plants that apply ferric and aluminum ions during the treatment process.

Although the addition of Fe^{3+} coagulant is beneficial for solids and phosphorous removal from wastewaters, coagulants have been shown to effect viral particles within wastewater, which may be problematic for the quantification of viral genomic measurements from wastewaters. In particular, earlier wastewater-based epidemiology studies have applied an "aluminum hydroxide adsorption-precipitation" method to concentrate for SARS-CoV-2 RNA measurements in wastewater with low solids (post-grit wastewater) (Bar-Or et al., 2020; Barril et al., 2021; Randazzo et al., 2020b, a). Ferric-based precipitation

has also been used in previous wastewater surveillance studies to effectively concentrates viruses from municipal wastewaters (Farrah and Preston, 1985; John et al., 2011; Payment et al., 1984; Randazzo et al., 2019; Sobsey et al., 1997). However, evidence that wastewater samples contaminated with ferric and aluminum ions were found to interfere with qPCR amplification for the detection of viruses (Combs et al., 2015; Dalecka and Mezule, 2018; Kuffel et al., 2021), and could cause false-negative results (Graham et al., 2021; Kitajima et al., 2018; Rock et al., 2010; Schrader et al., 2012), which were not previously considered in the earlier WWS studies. Hence, a knowledge gap regarding the effects of coagulation in primary sludge clarifiers on SARS-CoV-2 and PMMoV wastewater measurements exists, and it is necessary to further understand wastewater surveillance as a means of community prevalence of COVID-19 or incidence in communities. An additional factor that may indirectly influence SARS-CoV-2 and PMMoV RNA detection sensitivity due to the addition of coagulants is the associated decrease in primary sludge pH that occurs when a metal-based coagulant is added (Crittenden et al., 2012). Enteric viruses in wastewater, including nonenveloped viruses, increase their propensity for binding to wastewater colloids at lower pH due to associated changes in ionic strength and surface charges at low pH values (Walshe et al., 2010; Ye et al., 2016). The effects of trivalent metal coagulants and associated pH changes on the partitioning of SARS-CoV-2 and PMMoV viruses between the solids phase and the liquid phase have not been previously explored.

The implications of coagulation in primary clarifiers on the measurement of SARS-CoV-2 and PMMoV RNA in wastewaters remains unknown and needs to be understood to improve the ability of SARS-CoV-2 WWS to estimate the incidence of community COVID-19 disease. Further, by exploring the impact of ferric sulfate (Fe^{3+}) addition, a common primary sludge coagulant, on SARS-CoV-2 RNA and PMMoV RNA targets in wastewaters will improve our understanding of the partitioning of these biological targets in primary sludge wastewaters. The specific objectives of this study are to quantify the effects of Fe^{3+} and the corresponding pH changes on N1 and N2 SARS-CoV-2 gene region measurements as well as PMMoV measurements in primary sludge wastewaters and to use the results of Fe^{3+} addition on SARS-CoV-2 RNA and PMMoV RNA measurements in primary sludge to advance the current understanding of the partitioning of these targets in primary sludge wastewaters.

2 Materials and Methods

2.1 Wastewater source and collection

A total of 22.5 L of post-grit influent wastewater was collected on Feb. 22nd, Mar. 23rd, and May 2nd, 2021, from the City of Ottawa's (Ontario, Canada) WRRF, Robert O. Pickard Environmental Centre (ROPEC). 24-hour composite samples were collected using an ISCO 6700 series sampler (Teledyne ISCO Lincoln, NE, USA). The Ottawa WRRF treats wastewater collected from approximately 936,382 people and has an average wastewater flow rate of 545 million litres per day. Post-grit influent samples were collected in this study for various coagulant concentrations to be added to the harvested post-grit wastewaters to produce primary sludge samples of various coagulant concentrations. Samples were

immediately transported to the laboratory for storage following collection. During transportation, the samples were kept cold on ice, and they were then stored at 4°C in a refrigerator for a maximum of 24 hours before processing.

The physico-chemical characteristics of the post-grit influent samples were measured by the city of Ottawa WRRF laboratory as per standard methods common to wastewaters (APHA American Public Health Association, 2017). These characteristics include volatile suspended solids (VSS), total suspended solids (TSS), carbonaceous biological oxygen demand (cBOD), chemical oxygen demand (COD), total Kjeldahl nitrogen (TKN), and conductivity.

2.2 Jar tests

Jar testing of wastewaters is commonly performed to simulate primary clarification and coagulation processes at a lab-scale(American Water Works Association, 2011; Xiao et al., 2008). Coagulation of post-grit influent was performed in a series of jar tests at ferric sulfate dosages of 0, 5, 15, 30, and 60 mg/L as Fe^{3+}, with each dosage replicated three times for data quality assurance. To ensure that each jar-test replicate contained the same quantity of wastewater solids, the total solids (TS) was measured in each of the jar test beakers. Prior to dosing the post-grit wastewater samples with ferric sulfate, a 10 mL pipettor with a broad pipette tip was used to collect 20 mL of the homogenized post-grit wastewater sample from each beaker into a separate 75 mL aluminum weighing dish (Fisher Scientific, PA, USA) that was massed prior to use and labelled for each sample. The weighing dishes were then left in a furnace (VWR International, PA, USA) at 133°C for at least 24 hrs so that only the total solids would remain in the weighing dishes. An identical procedure was undertaken to measure the TS in the wastewater after the 30 min sedimentation period without resuspension of the settled solids. The weighting dishes were massed once more after removing from the furnace and the TS concentration (mg/L) for each sample replicate, before and after coagulation, was calculated by taking the difference in masses of the empty weighing dishes and weighing dishes with TS.

2.2.1 Effect of ferric sulfate dosing on SARS-CoV-2 and PMMoV viral measurements

Post-grit influent wastewaters harvested from the Ottawa WRRF on Feb. 22nd, 2021, were dosed with ferric sulfate ($Fe_2(SO_4)_3$) solution and mixed within conventional jar test apparatus (Orbeco-Hellige six-paddle stirrer, FL, USA) at distinct five concentrations of 0, 5, 15, 30 and 60 mg/L of Fe^{3+} to produce settled solids that simulate primary sludge and subsequently to be analyzed for SARS-CoV-2 and PMMoV viral measurements. Each of these five concentrations were prepared in triplicate, resulting in 15 samples analyzed from the wastewater harvested on Feb. 22nd, 2021. This procedure was replicated once more with the post-grit influent wastewaters collected on Mar. 23rd, and May 2nd, 2021, and dosed with ferric sulfate at 0 and 60 mg/L of Fe^{3+} and were run as complete test replicates to the Feb 22nd samples to ensure that variations in wastewater samples did not alter the findings of the study. Each jar test consisted of a rapid mixing, slow mixing, and sedimentation step within the test apparatus to simulate conventional primary clarification and coagulation processes (Fig. 1). The post-grit samples were first

well homogenized (well-mixed samples to resuspend solids within the wastewater matrix) and then 500 mL of the samples were aliquoted into disinfected jar test B-KER^2 laboratory 1000 mL beakers (Phipps & Bird PN 7790630, VA, USA). The beakers and the paddle stirrers were disinfected with 5% bleach solution (5 min contact time) and 70% ethanol (5 min contact) and then rinsed with tap water prior to use. Ferric sulfate coagulant solution was prepared from acidified ferric sulfate stock coagulant (12% concentration as Fe^{3+}). The coagulation process of the post-grit samples was then initiated by undergoing rapid mixing at 100 rotations per minute (RPM) for one minute immediately after the beakers with the 500 mL of homogenized samples were dosed with ferric sulfate, followed by 15 min of slow mixing at 40 RPM. Immediately thereafter, the mixing pedals were removed from the beakers for a 30 min sedimentation period to allow large flocs to settle down. Finally, a 10 mL pipettor with a broad (disposable) pipette tip was used to preferentially aspirate 40 mL of the settled solids fraction at the bottom of the beakers into a 40 mL disinfected centrifuge tube.

2.2.2 Effect of associated pH change on SARS-CoV-2 and PMMoV viral measurements

An identical procedure to the jar test method described above (Fig. 1) was also conducted in this study to determine the indirect effects of pH changes associated with ferric sulfate coagulant dosing on SARS-CoV-2 and PMMoV measurements in post-grit influent wastewaters. Jar test beakers with the same collected post-grit influent wastewaters on Feb 22nd, 2021, were slowly dosed with 1M hydrochloric acid (HCl) in place of ferric sulfate. These tests allowed for the effects of changes in the wastewater pH on SARS-CoV-2 and PMMoV due to ferric sulfate dosing to be isolated from the effects of the addition of ferric ion (Fe^{3+}). Immediately after the rapid mixing, slow mixing, and the 30 min sedimentation of the post-grit wastewater collected on Feb. 22nd with 0, 5, 15, 30, and 60 mg/L as Fe^{3+}, the wastewater pH for each sample replicate was measured using an HQ430d pH meter (Hach, CO, USA). As there was a minimal change in pH between each ferric sulfate concentration, only the pH for wastewater without coagulant (average pH of 7.6 ± 0.1) and wastewater with 60 mg/L as Fe^{3+} (average pH of 6.6 ± 0.2) were quantified. Three beakers with 500 mL of homogenized post-grit samples collected on Feb 22nd were dosed slowly with 1M HCl until a pH of 6.6 was reached (HQ430d pH meter, CO, USA), which was equivalent to the average pH recorded during dosing to 60 mg/L as Fe^{3+}, while an additional three post-grit samples collected on Feb. 22nd remained untreated to maintain a pH of 7.6; equivalent to the 0 mg/L as Fe^{3+} dosing. Following the 1 min rapid mixing at 100 rpm, 15 min slow mixing at 40 rpm, and 30 min sedimentation period, 40 mL of the settled solids were aspirated in a 40 mL centrifuge tube and were processed immediately for viral extraction and RT-qPCR quantification. The effect of pH change on SARS-CoV-2 and PMMoV measurements was only conducted for the aliquoted post-grit samples from Feb. 22nd, 2021, as results show no notable effects on the PMMoV-normalized SARS-CoV-2 measurements and were isolated from the effects of the coagulation process with ferric sulfate.

2.2.3 Effect of ferric sulfate dosing on SARS-CoV-2 and PMMoV partitioning in wastewaters

This study further investigates the influence of ferric sulfate addition on the partitioning of SARS-CoV-2 and PMMoV RNA between the solids and liquid fractions of wastewaters. An identical jar-testing procedure to the above-described experiments (Sections 2.2 and 2.2.1) was performed with post-grit wastewater samples collected on Mar. 23rd and May 2nd, 2021 at a dosage of 0 and 60 mg/L as Fe^{3+} with each concentration being performed in triplicate, resulting in a total of 12 samples analysed for both SARS-CoV-2 and PMMoV. The SARS-CoV-2 and PMMoV viral measurements in the wastewater from both days were analyzed in both the settled solids fraction and the supernatant (liquid) fraction. After the 1 min rapid mixing, 15 min slow mixing, and the 30 min sedimentation period for all samples and prior to aspiration of the settled solids, a 10 mL pipettor was used to collect 15 mL of the supernatant at different depths of the beaker to homogenize the supernatant samples, but without resuspension of the settled solids. Supernatant samples were collected before collecting the settled solids samples after the 30 min sedimentation period to ensure no resuspension of solid wastewater particles into the supernatant samples such that subsequent SARS-CoV-2 and PMMoV measurements are from the liquid phase of the wastewater only. From the jar test conducted for the post-grit wastewater collected on Mar. 23rd, 2021, supernatant samples were only collected from the beakers directly after the 30 min sedimentation period (settled supernatant), resulting in 6 supernatant samples that were processed in parallel with the 6 settled solids samples for viral extraction and RT-qPCR amplification, resulting in a total of 12 samples. As for the jar test conducted for post-grit wastewater collected on May 2nd, 2021, the resulting supernatant from the centrifugation (centrifuged supernatant) of the subsequent solids pellet was also collected in addition to the settled supernatant to investigate whether SARS-CoV-2 and PMMoV viral particles are localized within the supernatant post-centrifugation, resulting in 12 supernatant samples that were processed in parallel with the 6 settled solids samples from May 2nd post-grit wastewater for a total of 18 samples (Fig. 2). The supernatant samples were processed for viral extraction and RT-qPCR quantification using the same protocol that was applied for the solids pellet.

2.3 Enrichment, extraction and RT-qPCR quantification of SARS-CoV-2 and PMMoV

The settled solids samples were concentrated by centrifuging the samples at 10,000 × g for 45 min at 4°C. The supernatant was decanted to isolate the settled solids fraction and the sample was centrifuged once more at 10,000 × g for 5 min at 4°C to isolate the centrifuged solids pellet (also referred to as wet solids). Sample pellets inside the 40 mL centrifuge were massed and the total pellet weight was recorded, and then 0.250 ± 0.05 g of the sample pellets were immediately processed for viral extraction and RT-qPCR quantification. RNA was extracted using a Qiagen RNeasy PowerMicrobiome extraction kit (PN 26000-50, MD, USA) on a QIAcube Connect automated extraction platform with a modified methodology previously described using the RNeasy PowerMicrobiome Kit (Qiagen, Germantown, MD) (D'Aoust et al., 2021b, c). RT-qPCR quantification was performed for the SARS-CoV-2 N1 and N2 gene regions, as well as the replication-associated gene region of the pepper mild mottle virus (PMMoV), where measurements of PMMoV involved 1/10 dilution of samples. Each PCR reaction well consisted of 1.5 µL of RNA template and each sample was analyzed in triplicates; referred to as "biological replicates" throughout this study. The primer and probe combinations that were used in this study are shown in Table 1S (Supplementary

Material). To check for inhibition, the samples were diluted by a factor of four and then a factor of ten and were compared with undiluted samples for corresponding decreases in PMMoV measurements. The assay limit of detection (ALOD, ≥ 95% detection) was determined to be approximately 2 copies/reaction (D'Aoust et al., 2021b). To avoid contamination, RNA extraction and RT-qPCR were performed in separate laboratories in Class 2 biosafety cabinets. The resulting SARS-CoV-2 N1 and N2 viral measurements, as well as PMMoV viral measurements in this study, are represented as N1, N2, and PMMoV genomic copies (or copies) per gram of extracted wastewater concentrated solids (0.250 ± 0.05 g) and N1, N2 and PMMoV copies per sample-volume basis (500 mL). The PMMoV-normalized SARS-CoV-2 viral measurements measured in wastewater during this study are expressed as N1 and N2 copies/copies of PMMoV.

2.4 Statistical analysis

To test for statistically significant changes between SARS-CoV-2 N1 and N2 measurements, as well as PMMoV measurements of the differing five ferric sulfate dosed concentrations in the resulting settled solids fraction and the supernatant fractions, a one-way analysis of variance (ANOVA) was performed with a *p*-value of 0.05 or lower indicating statistical significance. ANOVA was also used to determine the statistical significance of SARS-CoV-2 and PMMoV RNA viral detection due to a change in pH. Throughout this study, the linear association (R^2) between the SARS-CoV-2 N1 and N2 and PMMoV viral signal measurements, and the ferric sulfate dosed concentrations, were determined cumulatively with respect to all individual resulting data.

3 Results and Discussion

3.1 Characteristics of Ottawa post-grit influent wastewater

The physico-chemical characteristics of the post-grit influent wastewater samples collected from the Ottawa WRRF exhibited low variations across the three distinct sampling dates (Table 1). It is noted that wastewater parameters are measured every second day at the Ottawa WRRF, and the parameters corresponding to the sampling date of Feb. 22nd were measured on that day, while the parameters corresponding to the additional sampling dates of Mar. 23rd and May 2nd of this study were calculated by averaging the wastewater measurements performed on the day prior and following those sampling dates As such, the wastewater characteristics shown for Feb. 22nd in Table 1 are a single date measurement and do not show standard deviations, while the wastewater characteristics shown for Mar. 23rd and May 2nd are the average of two measurements and hence show standard deviations.

Table 1
Physico-chemical characteristics of post-grit influent samples collected at the Ottawa (Ontario, Canada) WRRF on the sampling dates during this study.

Wastewater characteristics	Feb. 22nd	Mar. 22nd – 24th (avg. ± standard dev.)	May 1st – 3rd (avg ± standard dev.)
VSS (mg/L)	270	219 ± 52	353 ± 152
cBOD (mg/L)	201	164 ± 7	243 ± 79
COD (mg/L)	660	488 ± 77	693 ± 302
TSS (mg/L)	323	289 ± 72	348 ± 53
TKN (mg/L)	53.7	36.6 ± 0.9	44.3 ± 4.5
Conductivity (µS/cm)	1,234	1,606 ± 143	1,392 ± 51

The daily COVID-19 positive cases (five-day midpoint average in brackets) reported by Ottawa Public Health (OPH) on Feb. 22nd was 31 (46.0 ± 12.3) (Table 2), and on Mar. 23rd, and May 2nd, 2021 were 95 (88.6 ± 22.8), and 118 (121.2 ± 21.8), respectively (Table 2S in Supplemental Material). The daily COVID-19 positive cases (five-day midpoint average in brackets) between June 1st, 2020, through May 4th, 2021, ranged from 0 to 682 (62.2 ± 82). The daily percentage test positivity (five-day midpoint average) reported by the Ontario Laboratories Information System (OLIS) on Feb. 22nd, Mar. 23rd, and May 2nd, 2021, were 1.4% (2.1%), 3.3% (4.0%), and 6.9% (8.2%), respectively (Table 2). The daily percentage test positivity (five-day midpoint average in brackets) from Jun. 1st, 2020, through May 2nd, 2021, ranged from 0.0–16.8% (2.6% ± 2.9%).

Table 2

Viral signal measurements (average ± standard deviation of biological replicates) from post-grit influent wastewater samples collected on Feb. 22nd, 2021, from this study at Ottawa (Ontario, Canada) WRRF with no coagulant.

Copies/g	**N1**	$3.0 \times 10^3 \pm 8.7 \times 10^2$
	N2	$3.0 \times 10^3 \pm 7.2 \times 10^2$
	PMMoV	$1.0 \times 10^7 \pm 1.1 \times 10^6$
Copies/L	**N1**	$4.3 \times 10^3 \pm 1.3 \times 10^3$
	N2	$4.3 \times 10^3 \pm 1.1 \times 10^3$
	PMMoV	$1.5 \times 10^7 \pm 2.5 \times 10^6$
Copies/copies PMMoV	**N1**	$2.9 \times 10^{-4} \pm 7.9 \times 10^{-5}$
	N2	$2.9 \times 10^{-4} \pm 7.6 \times 10^{-5}$
Daily COVID-19 positive cases		31
Daily COVID-19 percent positivity		1.4%

3.2 Effect of ferric sulfate coagulant on SARS-CoV-2 and PMMoV viral signal measurements

The effects ferric sulfate dosing at 0, 5, 15, 30, and 60 mg/L as Fe^{3+} on the detection of SARS-CoV-2 N1 and N2 and PMMoV viral measurements in settled solids were investigated, with RT-qPCR analysis of the resulting solids pellets for each biological replicate displayed oscillations between 1460 and 6700 N1 and N2 copies/g without a significant change in trend across all five Fe^{3+} concentrations ($p = 0.200$ and $p = 0.313$) with a very weak linear relation ($R^2 = 0.008$ and $R^2 = 0.031$) (Fig. 3A and B, respectively). As such, findings suggest no significant effects of ferric sulfate coagulant dosage on N1 copies/g measurements (Fig. 3A) and in N2 copies/g measurements, except for the N2 copies/g measurements at 5 mg/L Fe^{3+} which is a likely outlier (Fig. 3B). The N1 and N2 copies/L measurements for each biological replicate ranged between 2.1×10^3 and 1.4×10^4 N1 and N2 copies/L and exhibited a statistically significant change across the five Fe^{3+} ($p < 0.05$) and a very weak linear relation ($R^2 = 0.216$ and $R^2 = 0.038$) remains between the increasing Fe^{3+} concentrations and the SARS-CoV-2 N1 and N2 copies/L (Fig. 3D and E, respectively). This weak linear relation is likely attributed to the differing pellet weights obtained throughout all the five Fe^{3+} concentrations (Table 3S in Supplementary Material). An experimental replicate with ferric sulfate dosages of 0 and 60 mg/L as Fe^{3+} similarly displayed no significant change in the N1 and N2 copies/g trend ($p = 0.557$ and $p = 0.519$) with a very weak linear relation ($R^2 = 0.090$ and

R^2 = 0.033) (Fig. 1S A and B in Supplementary Material). Hence, ferric sulfate dosages exhibited no significant effect on the SARS-CoV-2 RNA viral measurements in settled solids.

PMMoV viral measurements in settled solids from the post-grit wastewater that was collected from the Ottawa WRRF on Feb. 22nd, 2021, were detected at all five Fe^{3+} concentrations. Unlike the observations for the N1 and N2 gene region measurements, coagulation with ferric sulfate significantly affected the PMMoV viral signal measurements in the settled solids (Fig. 3C and F). Measurements represented in PMMoV copies/g and PMMoV copies/L ranged from 8.8 x 10^6 to 4.0 x 10^7 and 1.2 x 10^7 to 8.2 x 10^7, respectively, displayed a statistically significant increase with increasing Fe^{3+} concentrations ($p < 0.05$) along with a strong linear dependence (R^2 = 0.843 and R^2 = 0.873, respectively) (Fig. 3C and F). Higher PMMoV measurements in wastewater were previously associated with higher fractions of solids in wastewater (Kitamura et al., 2021). However, in this study, the PMMoV copies/g and copies/L measurements have a stronger linear dependence on Fe^{3+} concentrations (R^2 = 0.843 and R^2 = 0.873) (Fig. 3C and F, respectively)) compared to the resulting settled solids pellet at all five Fe^{3+} concentrations (R^2 = 0.377 and R^2 = 0.638) (Fig. 2S A and B, respectively, in Supplemental Material). An additional experimental replicate with ferric sulfate dosage of 0 and 60 mg/L as Fe^{3+} similarly displayed a statistically significant increase with increasing Fe^{3+} concentrations ($p < 0.05$) along with a strong linear association (R^2 = 0.940 and R^2 = 0.915) (Fig. 1S C and F in Supplemental Material). Hence, the significant elevations of PMMoV viral measurements in the settled solids are more strongly associated with the increased coagulant concentration in the post-grit wastewater samples collected on Feb. 22nd, 2021. Consequently, the increased Fe^{3+} dosages were shown to significantly reduce the SARS-CoV-2 copies of N1 and N2 per copies of PMMoV-normalized measurements in the settled solids samples ($p < 0.05$) (Fig. 3G and H); this significant reduction in the PMMoV-normalized measurements ($p < 0.05$) was similarly observed the consecutive experimental replicate (Fig. 1S G and H). This suggests that coagulation with ferric sulfate could cause a significant under-representation of PMMoV-normalized SARS-CoV-2 viral measurements in settled solids in WWS applications.

It has been previously identified that the virus interactions with various solid surfaces is primarily governed by long range hydrophobic and electrostatic interactions between the viral capsid and the surfaces. Although short ranged Vander Wall's forces and stearic interactions affect the virus-solid interactions, they are, however, of secondary importance (Lee et al., 2016; Xagoraraki et al., 2014; Ye et al., 2016). Enveloped viruses, such as SARS-CoV-2 virion particles, have been shown to have a higher propensity to adsorb to wastewater solids compared to non-enveloped viruses, such as PMMoV virion particles, due to presence of the hydrophobic lipid bilayer membrane and S spike protein on the virus surface (Duan et al., 2020; Kampf et al., 2020; Kumar et al., 2021; Wang et al., 2022; Ye et al., 2016). Since PMMoV RNA was previously measured in both the wastewater solids fraction and the supernatant fraction (Kim et al., 2021; Kitamura et al., 2021), it is hypothesized that the observed change in PMMoV viral measurements associated with the increasing Fe^{3+} concentrations is likely attributed to alterations in electrostatic interactions between PMMoV virion particles and the settled wastewater solids. Change in

the virus' surface charge was also reported to affect their propensity for binding to wastewater colloids from the liquid phase (Walshe et al., 2010; Ye et al., 2016). Virus' surface charges are influenced either by: i) change in the virion particle isoelectric point (pH at which the viral particles have zero net electrical potential) due to pH change (Walshe et al., 2010) or ii) by the neutralization of wastewater colloids during the coagulation process (Crittenden et al., 2012), which is hypothesized to increase electrostatic interactions between the PMMoV virion particles in the liquid phase and wastewater colloids. In this study, those two hypotheses are explored by i) testing the effects of the consecutive pH decrease associated with the increased Fe^{3+} dosages in the post-grit samples, and ii) by measuring the SARS-CoV-2 and PMMoV RNA in the supernatant fractions of the wastewater at increasing Fe^{3+} concentrations.

3.3 Effect of pH change on SARS-CoV-2 and PMMoV viral signal measurements

This study further explored whether the pH decrease associated with the increased Fe^{3+} dosages affects SARS-CoV-2 and PMMoV copies independent of direct Fe^{3+} effects. All five of the post-grit wastewaters demonstrated that pH values decreased after Fe^{3+} addition from 7.6 ± 0.1 (at 0 mg/L Fe^{3+}) to 6.6 ± 0.2 (at 60 mg/L Fe^{3+}), which lie within the optimal operating pH range of 5.0–8.5 for ferric precipitation during enhanced primary clarification (Crittenden et al., 2012). Measurements of N1 and N2 copies/g oscillating between 1500 and 4880 copies/g showed no statistically significant change between the two pH conditions ($p = 0.173$ and $p = 0.536$) (Fig. 4A and B, respectively). However, measurements of PMMoV copies/g showed a statistically significant decrease in the samples from $9.0 \times 10^6 \pm 3.2 \times 10^6$ at pH 6.6 to $5.5 \times 10^6 \pm 1.7 \times 10^6$ at pH 7.6 ($p < 0.05$) (Fig. 4C). This finding runs contrary to the original hypothesis that reducing the sample pH would result in a higher PMMoV viral signal in solids since viral particles reportedly bind better to wastewater colloids at lower pH due to a reduction in the negative charge of the virus (Walshe et al., 2010). PMMoV viral particles are negatively charged at an environmental pH above 3.8 (Charles P. Gerba, 1984; Kitajima et al., 2018; Michen and Graule, 2010; Shirasaki et al., 2017; Vega, 2006; Wetter et al., 1984); thus, PMMoV surface charge at the sample with pH 7.6 would likely be more negatively charged than at sample with pH 6.6. Since wastewater solids are usually negatively charged as well, it would be expected that PMMoV RNA in samples with pH 6.6 (less negative surface charge) to have better binding to wastewater solids. However, it was found in previous studies that wastewater acidification could reduce adsorption of nonenveloped viruses (similar to PMMoV) in wastewater solids due to possible degradation or alteration in the integrity of the virus or wastewater flocs (Yang et al., 2022). Despite these changes in the PMMoV RNA measurements, the PMMoV-normalized SARS-CoV-2 N1 and N2 gene regions associated with these measurements are shown to not be significantly affected by this change in the measured PMMoV in the solids (Fig. 4D and E). Therefore, the pH decrease associated with the Fe^{3+} addition, isolated from the effects of Fe^{3+} itself, shows no statistical change in the PMMoV-normalized SARS-CoV-2 measurements in the wastewater solids.

3.4 Effect of ferric sulfate dosing on partitioning of PMMoV measurements between wastewater solids and supernatant

In post-grit wastewater influent collected on March 23rd and May 3rd, the SARS-CoV-2 RNA was exclusively detected in the wet solids fraction of the partitioning experiments with negligible detection of the signal in the settled supernatant and centrifuged supernatant fractions in both the untreated and treated samples by the coagulant (Fig. 5A). PMMoV RNA was similarly found to be enriched in the wet solids fraction of the post-grit wastewater (Fig. 5B); this is consistent with the previous finding that measured significantly higher PMMoV RNA in wastewater solids fraction compared to the liquid fraction (Kim et al., 2021). Solids from post-grit samples that were not treated by coagulant were shown to contain 96.35% ± 0.67% of the total PMMoV copies (Fig. 5B). Partitioning of PMMoV viral particles could still be observed in the samples treated with 60 mg/L Fe^{3+} for which an additional 3.48% ± 0.48% of total PMMoV viral copies transferred from the unsettled and settled supernatant fractions to the solids fraction; as such, when treated with 60 mg/L as Fe^{3+} dosage, the solids fraction contained 99.83% ± 0.11% of the total PMMoV biomass (Fig. 5B). With PMMoV being largely localized in the solids phase, this makes it an effective normalizing biomarker for the SARS-CoV-2 N1 and N2 gene regions in WWS. Normalization against PMMoV in WWS applications is particularly important as it better reflects the community prevalence of COVID-19 infections by accounting for variations in wastewater physico-chemical properties, fecal mass flux, and PCR amplification (D'Aoust et al., 2021b; Graham et al., 2021; Kitamura et al., 2021; Wolfe et al., 2021; Wu et al., 2021). Conclusion and Recommendations

Over the past 41 months since the detection of the first COVID-19 cases in December 2019, WWS has emerged as an effective disease surveillance tool for monitoring active COVID-19 cases (Ahmed et al., 2020; Arora et al., 2020; Bivins et al., 2020; D'Aoust et al., 2021a; Gonzalez et al., 2020; La Rosa et al., 2021; Mao et al., 2020; McClary-Gutierrez et al., 2021; Medema et al., 2020; Polo et al., 2020; Randazzo et al., 2020a, 2020b; Sims and Kasprzyk-Hordern, 2020; Thompson et al., 2020; Wu et al., 2020). In this investigation, the effect of the commonly used metal coagulant Fe^{3+} on SARS-CoV-2 and PMMoV viral measurements of primary sludge wastewaters was examined for potential implications on the effectiveness of WWS using primary sludge samples. Coagulation via the addition of Fe^{3+} did not significantly influence the average measurements of SARS-CoV-2 N1 and N2 viral copies per gram of wet wastewater solids or per liter of wastewater. However, the PMMoV measurement per wet wastewater solids showed a significantly higher measurement at elevated and with increasing concentrations of Fe^{3+}. Indirect pH reduction associated with adding ferric sulfate was not associated with trends observed for PMMoV copies and had no significant impact on PMMoV-normalized viral N1 and N2 copies. This observation is more likely attributed to possible changes in electrostatic interactions between PMMoV RNA particles and the settled wastewater solids associated with ferric sulfate addition. Ultimately, this change in PMMoV copies may significantly affect the normalization of SARS-CoV-2 viral copies in wastewater using PMMoV at elevated concentrations of Fe^{3+} and hence may result in an underestimation of the community prevalence of COVID-19 through WWS of the disease.

4 Conclusion and Recommendations

Over the past 41 months since the detection of the first COVID-19 cases in December 2019, WWS has emerged as an effective disease surveillance tool for monitoring active COVID-19 cases (Ahmed et al., 2020; Arora et al., 2020; Bivins et al., 2020; D'Aoust et al., 2021a; Gonzalez et al., 2020; La Rosa et al., 2021; Mao et al., 2020; McClary-Gutierrez et al., 2021; Medema et al., 2020; Polo et al., 2020; Randazzo et al., 2020a, 2020b; Sims and Kasprzyk-Hordern, 2020; Thompson et al., 2020; Wu et al., 2020). In this investigation, the effect of the commonly used metal coagulant Fe3+ on SARS-CoV-2 and PMMoV viral measurements of primary sludge wastewaters was examined for potential implications on the effectiveness of WWS using primary sludge samples. Coagulation via the addition of Fe3+ did not significantly influence the average measurements of SARS-CoV-2 N1 and N2 viral copies per gram of wet wastewater solids or per liter of wastewater. However, the PMMoV measurement per wet wastewater solids showed a significantly higher measurement at elevated and with increasing concentrations of Fe3+. Indirect pH reduction associated with adding ferric sulfate was not associated with trends observed for PMMoV copies and had no significant impact on PMMoV-normalized viral N1 and N2 copies. This observation is more likely attributed to possible changes in electrostatic interactions between PMMoV RNA particles and the settled wastewater solids associated with ferric sulfate addition. Ultimately, this change in PMMoV copies may significantly affect the normalization of SARS-CoV-2 viral copies in wastewater using PMMoV at elevated concentrations of Fe3+ and hence may result in an underestimation of the community prevalence of COVID-19 through WWS of the disease.

Declarations

Acknowledgements

The authors wish to acknowledge the help and assistance of the University of Ottawa, the Ottawa Hospital, the Children's Hospital of Eastern Ontario, the Children's Hospital of Eastern Ontario's Research Institute, Public Health Ontario and all of their employees who were involved in this project. Their time, facilities, resources, and feedback are greatly appreciated.

Author Contributions

All authors contributed to the study conception and design as described below. The first draft of the manuscript was written by Nada Hegazy and all authors commented on previous versions of the manuscript. All authors read and approved the final manuscript.

Nada Hegazy: experimental work, investigation, formal analysis, writing, review and editing.

Xin Tian: experimental work, review and editing

Patrick M. D'Aoust: experimental work, review and editing

Lakshmi Pisharody: investigation, review and editing

Syeda Tasneem Towhid: experimental work, review and editing

Élisabeth Mercier: review and editing

Zhihao Zhang: experimental work, review and editing

Shen Wan: review and editing

Ocean Thakali: review and editing

Md Pervez Kabir: review and editing

Wanting Fang: review and editing

Tram B. Nguyen: review and editing

Nathan T. Ramsay: review and editing

Alex E. MacKenzie: methodology, validation, review and editing, funding acquisition

Tyson E. Graber: review and editing

Stéphanie Guilherme: validation, supervision, review and editing

Robert Delatolla: methodology, validation, supervision, writing – review and editing, funding acquisition

Funding

This research was supported by the Province of Ontario's Wastewater Surveillance Initiative (WSI). It was also supported by a CHEO (Children's Hospital of Eastern Ontario) CHAMO (Children's Hospital Academic Medical Organization) grant, which was awarded to Dr. Alex E. MacKenzie.

Availability of Data and Materials

All data and materials analyzed during this study are included in this published article.

Ethical Approval

Not applicable.

Consent to Participate

Not applicable.

Consent to Publish

Not applicable.

Declaration of Competing Interests

The authors declare that no competing financial interests or personal relationships influenced the work reported in this manuscript.

References

1. Ahmed, W., Angel, N., Edson, J., Bibby, K., Bivins, A., O'Brien, J.W., Choi, P.M., Kitajima, M., Simpson, S.L., Li, J., Tscharke, B., Verhagen, R., Smith, W.J.M., Zaugg, J., Dierens, L., Hugenholtz, P., Thomas, K. V., Mueller, J.F., 2020. First confirmed detection of SARS-CoV-2 in untreated wastewater in Australia: A proof of concept for the wastewater surveillance of COVID-19 in the community. Sci. Total Environ. 728, 138764. https://doi.org/10.1016/j.scitotenv.2020.138764
2. American Water Works Association, 2011. Operational Control of Coagulation and Filtration Processes AWWA MANUAL M37, Third Edit. ed. American Water Works Association, Denver, CO, USA.
3. APHA American Public Health Association, 2017. Standard Methods for the Examination of Water and Wastewater, 23rd ed. Washington, DC.
4. Arora, S., Nag, A., Sethi, J., Rajvanshi, J., Saxena, S., Shrivastava, S.K., Gupta, A.B., 2020. Sewage surveillance for the presence of SARS-CoV-2 genome as a useful wastewater based epidemiology (WBE) tracking tool in India. Water Sci. Technol. 82, 2823–2836. https://doi.org/10.2166/wst.2020.540
5. Balboa, S., Mauricio-Iglesias, M., Rodriguez, S., Martínez-Lamas, L., Vasallo, F.J., Regueiro, B., Lema, J.M., 2020. The fate of SARS-CoV-2 in WWTPs points out the sludge line as a suitable spot for monitoring. medRxiv 2020.05.25.20112706. https://doi.org/10.1101/2020.05.25.20112706
6. Bar-Or, I., Yaniv, K., Shagan, M., Ozer, E., Erster, O., Mendelson, E., Mannasse, B., Shirazi, R., Kramarsky-Winter, E., Nir, O., Abu-Ali, H., Ronen, Z., Rinott, E., Lewis, Y.E., Friedler, E., Bitkover, E., Paitan, Y., Berchenko, Y., Kushmaro, A., 2020. Regressing SARS-CoV-2 sewage measurements onto COVID-19 burden in the population: A proof-of-concept for quantitative environmental surveillance. medRxiv 1–11. https://doi.org/10.1101/2020.04.26.20073569
7. Barril, P.A., Pianciola, L.A., Mazzeo, M., Ousset, M.J., Jaureguiberry, M.V., Alessandrello, M., Sánchez, G., Oteiza, J.M., 2021. Evaluation of viral concentration methods for SARS-CoV-2 recovery from wastewaters. Sci. Total Environ. 756, 144105. https://doi.org/10.1016/j.scitotenv.2020.144105
8. Bivins, A., North, D., Ahmad, A., Ahmed, W., Alm, E., Been, F., Bhattacharya, P., Bijlsma, L., Boehm, A.B., Brown, J., Buttiglieri, G., Calabro, V., Carducci, A., Castiglioni, S., Cetecioglu Gurol, Z., Chakraborty, S., Costa, F., Curcio, S., De Los Reyes, F.L., Delgado Vela, J., Farkas, K., Fernandez-Casi, X., Gerba, C., Gerrity, D., Girones, R., Gonzalez, R., Haramoto, E., Harris, A., Holden, P.A., Islam, M.T., Jones, D.L.,

Kasprzyk-Hordern, B., Kitajima, M., Kotlarz, N., Kumar, M., Kuroda, K., La Rosa, G., Malpei, F., Mautus, M., McLellan, S.L., Medema, G., Meschke, J.S., Mueller, J., Newton, R.J., Nilsson, D., Noble, R.T., Van Nuijs, A., Peccia, J., Perkins, T.A., Pickering, A.J., Rose, J., Sanchez, G., Smith, A., Stadler, L., Stauber, C., Thomas, K., Van Der Voorn, T., Wigginton, K., Zhu, K., Bibby, K., 2020. Wastewater-Based Epidemiology: Global Collaborative to Maximize Contributions in the Fight against COVID-19. Environ. Sci. Technol. https://doi.org/10.1021/acs.est.0c02388

9. Carliell-Marquet, C., Smith, J., Oikonomidis, I., Wheatley, A., 2010. Inorganic profiles of chemical phosphorus removal sludge. Proc. Inst. Civ. Eng. Manag. 163, 65–77. https://doi.org/10.1680/WAMA.2010.163.2.65
10. CDC, 2020. Real-Time RT-PCR diagnostic panel for emergency use only. CDC EUA.
11. Charles P. Gerba, 1984. Applied and theoretical aspects of virus adsorption to surfaces. Adv. Appl. Microbiol. 30, 133–168.
12. Combs, L.G., Warren, J.E., Huynh, V., Castaneda, J., Golden, T.D., Roby, R.K., 2015. The effects of metal ion PCR inhibitors on results obtained with the Quantifiler® Human DNA Quantification Kit. Forensic Sci. Int. Genet. 19, 180–189. https://doi.org/10.1016/j.fsigen.2015.06.013
13. Cornel, P., Schaum, C., 2009. Phosphorus recovery from wastewater: needs, technologies and costs. Water Sci. Technol. 59, 1069–1076. https://doi.org/10.2166/WST.2009.045
14. Crittenden, J.C., Trussell, R.R., Hand, D.W., Howe, K.J., Tchobanoglous, G., 2012. MWH's water treatment : principles and design, Third. ed. John Wiley and Sons.
15. D'Aoust, P.M., Graber, T.E., Mercier, E., Montpetit, D., Alexandrov, I., Neault, N., Baig, A.T., Mayne, J., Zhang, X., Alain, T., Servos, M.R., Srikanthan, N., MacKenzie, M., Figeys, D., Manuel, D., Jüni, P., MacKenzie, A.E., Delatolla, R., 2021a. Catching a resurgence: Increase in SARS-CoV-2 viral RNA identified in wastewater 48 h before COVID-19 clinical tests and 96 h before hospitalizations. Sci. Total Environ. 770. https://doi.org/10.1016/j.scitotenv.2021.145319
16. D'Aoust, P.M., Mercier, E., Montpetit, D., Jia, J.J., Alexandrov, I., Neault, N., Baig, A.T., Mayne, J., Zhang, X., Alain, T., Langlois, M.A., Servos, M.R., MacKenzie, M., Figeys, D., MacKenzie, A.E., Graber, T.E., Delatolla, R., 2021b. Quantitative analysis of SARS-CoV-2 RNA from wastewater solids in communities with low COVID-19 incidence and prevalence. Water Res. 188, 116560. https://doi.org/10.1016/j.watres.2020.116560
17. D'Aoust, P.M., Towhid, S.T., Mercier, É., Hegazy, N., Tian, X., Bhatnagar, K., Zhang, Z., Mackenzie, A.E., Graber, T.E., Delatolla, R., 2021c. COVID-19 monitoring in rural communities: First comparison of lagoon and pumping station samples for wastewater-based epidemiology. Environ. Sci. Water Res. Technol. https://doi.org/https://doi.org/10.1016/j.scitotenv.2021.149618
18. Dalecka, B., Mezule, L., 2018. Study of potential PCR inhibitors in drinking water for Escherichia coli identification. Agron. Res. 16, 1351–1359. https://doi.org/10.15159/AR.18.118
19. Davis, M.L., 2010. Water and Wastewater Engineering: Design Principles and Practice. McGraw-Hill Education.

20. Dong, T., Shewa, W.A., Murray, K., Dagnew, M., 2019. Optimizing chemically enhanced primary treatment processes for simultaneous carbon redirection and phosphorus removal. Water (Switzerland) 11. https://doi.org/10.3390/w11030547
21. Duan, L., Zheng, Q., Zhang, H., Niu, Y., Lou, Y., Wang, H., 2020. The SARS-CoV-2 Spike Glycoprotein Biosynthesis, Structure, Function, and Antigenicity: Implications for the Design of Spike-Based Vaccine Immunogens. Front. Immunol. 11, 1–12. https://doi.org/10.3389/fimmu.2020.576622
22. ECCC, 2011. Municipal Water Use Report.
23. ECCC, 2010. Optimization Guidance Manual for Sewage Works .
24. EPA, U., 2022. Industrial Wastewater Treatment Technology Database (IWTT) | US EPA [WWW Document]. URL https://watersgeo.epa.gov/iwtt/guided-search (accessed 1.16.23).
25. European Environment Agency, 2022. Urban Waste Water Treatment Directive – reported data [WWW Document]. URL https://www.eea.europa.eu/data-and-maps/data/waterbase-uwwtd-urban-waste-water-treatment-directive-9 (accessed 1.16.23).
26. Farrah, S.R., Preston, D.R., 1985. Concentration of viruses from water by using cellulose filters modified by in situ precipitation of ferric and aluminum hydroxides. Appl. Environ. Microbiol. 50, 1502–1504. https://doi.org/10.1128/AEM.50.6.1502-1504.1985
27. Gonzalez, R., Curtis, K., Bivins, A., Bibby, K., Weir, M.H., Yetka, K., Thompson, H., Keeling, D., Mitchell, J., Gonzalez, D., 2020. COVID-19 surveillance in Southeastern Virginia using wastewater-based epidemiology. Water Res. 186, 116296. https://doi.org/10.1016/j.watres.2020.116296
28. Graham, K.E., Loeb, S.K., Wolfe, M.K., Catoe, D., Sinnott-Armstrong, N., Kim, S., Yamahara, K.M., Sassoubre, L.M., Mendoza Grijalva, L.M., Roldan-Hernandez, L., Langenfeld, K., Wigginton, K.R., Boehm, A.B., 2021. SARS-CoV-2 RNA in Wastewater Settled Solids Is Associated with COVID-19 Cases in a Large Urban Sewershed. Environ. Sci. Technol. 55, 488–498. https://doi.org/10.1021/acs.est.0c06191
29. Haramoto, E., Kitajima, M., Kishida, N., Konno, Y., Katayama, H., Asami, M., Akiba, M., 2013. Occurrence of pepper mild mottle virus in drinking water sources in Japan. Appl. Environ. Microbiol. 79, 7413–7418. https://doi.org/10.1128/AEM.02354-13
30. Jafferali, M.H., Khatami, K., Atasoy, M., Birgersson, M., Williams, C., Cetecioglu, Z., 2021. Benchmarking virus concentration methods for quantification of SARS-CoV-2 in raw wastewater. Sci. Total Environ. 755, 142939. https://doi.org/10.1016/J.SCITOTENV.2020.142939
31. John, S.G., Mendez, C.B., Deng, L., Poulos, B., Kauffman, A.K.M., Kern, S., Brum, J., Polz, M.F., Boyle, E.A., Sullivan, M.B., 2011. A simple and efficient method for concentration of ocean viruses by chemical flocculation. Environ. Microbiol. Rep. 3, 195–202. https://doi.org/10.1111/J.1758-2229.2010.00208.X
32. Kampf, G., Todt, D., Pfaender, S., Steinmann, E., 2020. Persistence of coronaviruses on inanimate surfaces and their inactivation with biocidal agents. J. Hosp. Infect. 104, 246–251. https://doi.org/10.1016/j.jhin.2020.01.022

33. Kim, S., Kennedy, L.C., Wolfe, M.K., Criddle, C.S., Duong, D.H., Topol, A., White, B.J., Kantor, R.S., Nelson, K.L., Steele, J.A., Langlois, K., Griffith, J.F., Zimmer-Faust, A.G., McLellan, S.L., Schussman, M.K., Ammerman, M., Wigginton, K.R., Bakker, K.M., Boehm, A.B., 2021. SARS-CoV-2 RNA is enriched by orders of magnitude in solid relative to liquid wastewater at publicly owned treatment works. medRxiv 2021.11.10.21266138. https://doi.org/10.1101/2021.11.10.21266138
34. Kitajima, M., Sassi, H.P., Torrey, J.R., 2018. Pepper mild mottle virus as a water quality indicator. npj Clean WaterClean Water 1. https://doi.org/10.1038/s41545-018-0019-5
35. Kitamura, K., Sadamasu, K., Muramatsu, M., Yoshida, H., 2021. Efficient detection of SARS-CoV-2 RNA in the solid fraction of wastewater. Sci. Total Environ. 763, 144587. https://doi.org/10.1016/j.scitotenv.2020.144587
36. Kuffel, A., Gray, A., Daeid, N.N., 2021. Impact of metal ions on PCR inhibition and RT-PCR efficiency. Int. J. Legal Med. 135, 63–72. https://doi.org/10.1007/s00414-020-02363-4
37. Kumar, M., Mazumder, P., Mohapatra, S., Kumar Thakur, A., Dhangar, K., Taki, K., Mukherjee, S., Kumar Patel, A., Bhattacharya, P., Mohapatra, P., Rinklebe, J., Kitajima, M., Hai, F.I., Khursheed, A., Furumai, H., Sonne, C., Kuroda, K., 2021. A chronicle of SARS-CoV-2: Seasonality, environmental fate, transport, inactivation, and antiviral drug resistance. J. Hazard. Mater. 405, 124043. https://doi.org/10.1016/j.jhazmat.2020.124043
38. La Rosa, G., Mancini, P., Bonanno Ferraro, G., Veneri, C., Iaconelli, M., Bonadonna, L., Lucentini, L., Suffredini, E., 2021. SARS-CoV-2 has been circulating in northern Italy since December 2019: Evidence from environmental monitoring. Sci. Total Environ. 750, 141711. https://doi.org/10.1016/j.scitotenv.2020.141711
39. Lee, M.T., Prudent, A., Marr, L.C., 2016. Partitioning of Viruses in Wastewater Systems and Potential for Aerosolization. Environ. Sci. Technol. Lett. 3, 210–215. https://doi.org/10.1021/ACS.ESTLETT.6B00105
40. Mao, K., Zhang, K., Du, W., Ali, W., Feng, X., Zhang, H., 2020. The potential of wastewater-based epidemiology as surveillance and early warning of infectious disease outbreaks. Curr. Opin. Environ. Sci. Heal. https://doi.org/10.1016/j.coesh.2020.04.006
41. McClary-Gutierrez, J.S., Mattioli, M.C., Marcenac, P., Silverman, A.I., Boehm, A.B., Bibby, K., Balliet, M., De Los Reyes, F.L., Gerrity, D., Griffith, J.F., Holden, P.A., Katehis, D., Kester, G., LaCross, N., Lipp, E.K., Meiman, J., Noble, R.T., Brossard, D., McLellan, S.L., 2021. SARS-CoV-2 Wastewater Surveillance for Public Health Action. Emerg. Infect. Dis. 27, E1–E9. https://doi.org/10.3201/EID2709.210753
42. Mckinnon, I., Pellegrino, M., Rak-Banville, J., Goss, C., Brant, B., Thorne, G., 2018. Pilot Testing an Alternative Coagulant for the Winnipeg Water Treatment Plant.
43. Medema, G., Heijnen, L., Elsinga, G., Italiaander, R., Brouwer, A., 2020. Presence of SARS-Coronavirus-2 RNA in Sewage and Correlation with Reported COVID-19 Prevalence in the Early Stage of the Epidemic in the Netherlands. Environ. Sci. Technol. Lett. 7, 511–516. https://doi.org/10.1021/acs.estlett.0c00357

44. Metcalf and Eddy, 2014. Wastewater Engineering - Treatment and Resource Recovery, 5th ed. McGraw-Hill Education, New York, US.
45. Michen, B., Graule, T., 2010. Isoelectric points of viruses. J. Appl. Microbiol. 109, 388–397. https://doi.org/10.1111/J.1365-2672.2010.04663.X
46. Pal, P., 2017. Chemical Treatment Technology, in: Industrial Water Treatment Process Technology. Butterworth-Heinemann, pp. 21–63. https://doi.org/10.1016/B978-0-12-810391-3.00002-3
47. Payment, P., Fortin, S., Trudel, M., 1984. Ferric chloride flocculation for nonflocculating beef extract preparations. Appl. Environ. Microbiol. 47, 591–592. https://doi.org/10.1128/AEM.47.3.591-592.1984
48. Peccia, J., Zulli, A., Brackney, D.E., Grubaugh, N.D., Kaplan, E.H., Casanovas-Massana, A., Ko, A.I., Malik, A.A., Wang, D., Wang, M., Warren, J.L., Weinberger, D.M., Arnold, W., Omer, S.B., 2020. Measurement of SARS-CoV-2 RNA in wastewater tracks community infection dynamics. Nat. Biotechnol. 38, 1164–1167. https://doi.org/10.1038/s41587-020-0684-z
49. Petala, M., Dafou, D., Kostoglou, M., Karapantsios, T., Kanata, E., Chatziefstathiou, A., Sakaveli, F., Kotoulas, K., Arsenakis, M., Roilides, E., Sklaviadis, T., Metallidis, S., Papa, A., Stylianidis, E., Papadopoulos, A., Papaioannou, N., 2021. A physicochemical model for rationalizing SARS-CoV-2 concentration in sewage. Case study: The city of Thessaloniki in Greece. Sci. Total Environ. 755, 142855. https://doi.org/10.1016/j.scitotenv.2020.142855
50. Polo, D., Quintela-Baluja, M., Corbishley, A., Jones, D.L., Singer, A.C., Graham, D.W., Romalde, J.L., 2020. Making waves: Wastewater-based epidemiology for COVID-19 – approaches and challenges for surveillance and prediction. Water Res. 186, 116404. https://doi.org/10.1016/j.watres.2020.116404
51. Randazzo, W., Cuevas-Ferrando, E., Sanjuán, R., Domingo-Calap, P., Sánchez, G., 2020a. Metropolitan wastewater analysis for COVID-19 epidemiological surveillance. Int. J. Hyg. Environ. Heal. 230. https://doi.org/10.1101/2020.04.23.20076679
52. Randazzo, W., Piqueras, J., Zoran Evtoski, ·, Sastre, G., Sancho, R., Gonzalez, C., Sánchez, G., 2019. Interlaboratory Comparative Study to Detect Potentially Infectious Human Enteric Viruses in Influent and Effluent Waters. Food Environ. Virol. 11, 350–363. https://doi.org/10.1007/s12560-019-09392-2
53. Randazzo, W., Truchado, P., Cuevas-Ferrando, E., Simón, P., Allende, A., Sánchez, G., 2020b. SARS-CoV-2 RNA in wastewater anticipated COVID-19 occurrence in a low prevalence area. Water Res. 181. https://doi.org/10.1016/j.watres.2020.115942
54. Rock, C., Alum, A., Abbaszadegan, M., 2010. PCR inhibitor levels in concentrates of biosolid samples predicted by a new method based on excitation-emission matrix spectroscopy. Appl. Environ. Microbiol. 76, 8102–8109. https://doi.org/10.1128/AEM.02339-09
55. Rosario, K., Symonds, E.M., Sinigalliano, C., Stewart, J., Breitbart, M., Petersburg, S., 2009. Pepper Mild Mottle Virus as an Indicator of Fecal Pollution. Appl. Environ. Microbiol. 75, 7261–7267. https://doi.org/10.1128/AEM.00410-09

56. Schrader, C., Schielke, A., Ellerbroek, L., Johne, R., 2012. PCR inhibitors – occurrence, properties and removal. J. Appl. Microbiol. 113, 1014–1026. https://doi.org/10.1111/J.1365-2672.2012.05384.X
57. Shewa, W.A., Dagnew, M., 2020. Revisiting chemically enhanced primary treatment of wastewater: A review. Sustainability 12, 1–19. https://doi.org/10.3390/SU12155928
58. Shirasaki, N., Matsushita, T., Matsui, Y., Murai, K., 2017. Assessment of the efficacy of membrane filtration processes to remove human enteric viruses and the suitability of bacteriophages and a plant virus as surrogates for those viruses. Water Res. 115, 29–39. https://doi.org/10.1016/j.watres.2017.02.054
59. Sims, N., Kasprzyk-Hordern, B., 2020. Future perspectives of wastewater-based epidemiology: Monitoring infectious disease spread and resistance to the community level. Environ. Int. https://doi.org/10.1016/j.envint.2020.105689
60. Sobsey, M.D., Gerba, C.P., Wallis, Craig, D Joseph L Melnick, A.N., C P Gerba, M.D., Wallis, C, Melnick, J.L., 1997. Concentration of enteroviruses from large volumes of turbid estuary water. Can. J. Microbiol. 23, 770–778.
61. Thompson, J.R., Nancharaiah, Y. V., Gu, X., Lee, W.L., Rajal, V.B., Haines, M.B., Girones, R., Ng, L.C., Alm, E.J., Wuertz, S., 2020. Making waves: Wastewater surveillance of SARS-CoV-2 for population-based health management. Water Res. 184, 116181. https://doi.org/10.1016/j.watres.2020.116181
62. Toronto Water, 2009. Update on the Supply Shortage of Iron Salts for Wastewater Treatment.
63. U.S. EPA, 2000. Wastewater Technology Fact Sheet - Chemical Precipitation, Environmental Protection Agency. Washington, DC.
64. Vega, E., 2006. Attachment and survival of viruses on lettuce (lactuca sativa l. Var. Capitata l.): Role of physicochemical and biotic factors. Texas A&M University.
65. Walshe, G.E., Pang, L., Flury, M., Close, M.E., Flintoft, M., 2010. Effects of pH, ionic strength, dissolved organic matter, and flow rate on the co-transport of MS2 bacteriophages with kaolinite in gravel aquifer media. Water Res. 44, 1255–1269. https://doi.org/10.1016/j.watres.2009.11.034
66. Wang, R., Alamin, M., Tsuji, S., Hara-Yamamura, H., Hata, A., Zhao, B., Ihara, M., Honda, R., 2022. Removal performance of SARS-CoV-2 in wastewater treatment by membrane bioreactor, anaerobic-anoxic-oxic, and conventional activated sludge processes. Sci. Total Environ. 851, 158310. https://doi.org/10.1016/J.SCITOTENV.2022.158310
67. Westhaus, S., Weber, F.A., Schiwy, S., Linnemann, V., Brinkmann, M., Widera, M., Greve, C., Janke, A., Hollert, H., Wintgens, T., Ciesek, S., 2021. Detection of SARS-CoV-2 in raw and treated wastewater in Germany – Suitability for COVID-19 surveillance and potential transmission risks. Sci. Total Environ. 751, 141750. https://doi.org/10.1016/J.SCITOTENV.2020.141750
68. Wetter, C., Conti, M., Altschuh, D., Tabillion, R., Regenmortel, M.H.V. van, 1984. Pepper Mild Mottle Virus, a Tobamovirus Infecting Pepper Cultivars in Sicily. Phytopathology 74, 405–420. https://doi.org/10.1094/phyto-74-405
69. Wolfe, M.K., Archana, A., Catoe, D., Coffman, M.M., Dorevich, S., Graham, K.E., Kim, S., Mendoza Grijalva, L., Roldan-Hernandez, L., Silverman, A.I., Sinnott-Armstrong, N., Vugia, D.J., Yu, A.T.,

Zambrana, W., Wigginton, K.R., Boehm, A.B., 2021. Scaling of SARS-CoV-2 RNA in Settled Solids from Multiple Wastewater Treatment Plants to Compare Incidence Rates of Laboratory-Confirmed COVID-19 in Their Sewersheds. Environ. Sci. Technol. Lett. 8, 398–404. https://doi.org/10.1021/acs.estlett.1c00184

70. Wu, F., Xiao, A., Zhang, J., Moniz, K., Endo, N., Armas, F., Bushman, M., Chai, P.R., Duvallet, C., Erickson, T.B., Foppe, K., Ghaeli, N., Gu, X., Hanage, W.P., Huang, K.H., Lee, W.L., Matus, M., McElroy, K.A., Rhode, S.F., Wuertz, S., Thompson, J., Alm, E.J., 2021. Wastewater Surveillance of SARS-CoV-2 across 40 U.S. states. medRxiv 1–13. https://doi.org/10.1101/2021.03.10.21253235
71. Wu, F., Zhang, J., Xiao, A., Gu, X., Lee, W.L., Armas, F., Kauffman, K., Hanage, W., Matus, M., Ghaeli, N., Endo, N., Duvallet, C., Poyet, M., Moniz, K., Washburne, A.D., Erickson, T.B., Chai, P.R., Thompson, J., Alm, E.J., 2020. SARS-CoV-2 Titers in Wastewater Are Higher than Expected from Clinically Confirmed Cases. Am. Soc. Microbiol. 5. https://doi.org/10.1128/msystems.00614-20
72. Xagoraraki, I., Yin, Z., Svambayev, Z., 2014. Fate of Viruses in Water Systems. J. Environ. Eng. 140, 04014020–1. https://doi.org/10.1061/(ASCE)EE.1943-7870.0000827
73. Xiao, F., Ma, J., Yi, P., Huang, J.C.H., 2008. Effects of low temperature on coagulation of kaolinite suspensions. Water Res. 42, 2983–2992. https://doi.org/10.1016/J.WATRES.2008.04.013
74. Yang, W., Cai, C., Dai, X., 2022. Interactions between virus surrogates and sewage sludge vary by viral analyte: Recovery, persistence, and sorption. Water Res. 210, 117995. https://doi.org/10.1016/j.watres.2021.117995
75. Ye, Y., Ellenberg, R.M., Graham, K.E., Wigginton, K.R., 2016. Survivability, Partitioning, and Recovery of Enveloped Viruses in Untreated Municipal Wastewater. Environ. Sci. Technol. 50, 5077–5085. https://doi.org/10.1021/ACS.EST.6B00876
76. Yeoman, S., Stephenson, T., Lester, J.., Perry, R., 1988. The Removal of Phosphorus During Wastewater Treatment: A Review. Environ. Pollut. 49, 183–233. https://doi.org/10.1016/0269-7491(88)90209-6.
77. Zulli, A., Pan, A., Bart, S.M., Crawford, F.W., Kaplan, E.H., Cartter, M., Ko, A.I., Sanchez, M., Brown, C., Cozens, D., Brackney, D.E., Peccia, J., 2021. Predicting daily COVID-19 case rates from SARS-CoV-2 RNA concentrations across a diversity of wastewater catchments. FEMS Microbes 2, 22. https://doi.org/10.1093/femsmc/xtab022

Figures

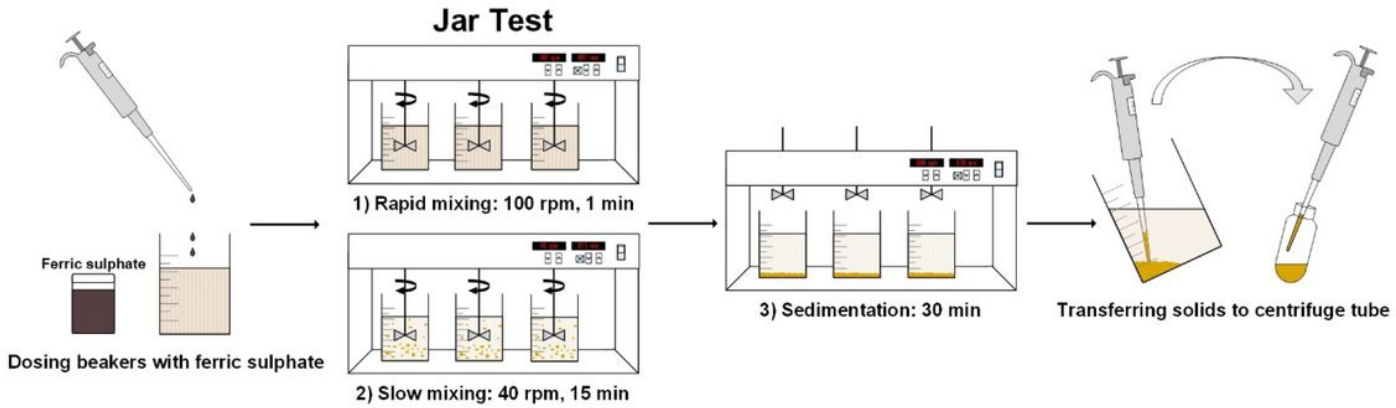

Figure 1

Jar test method used in this study

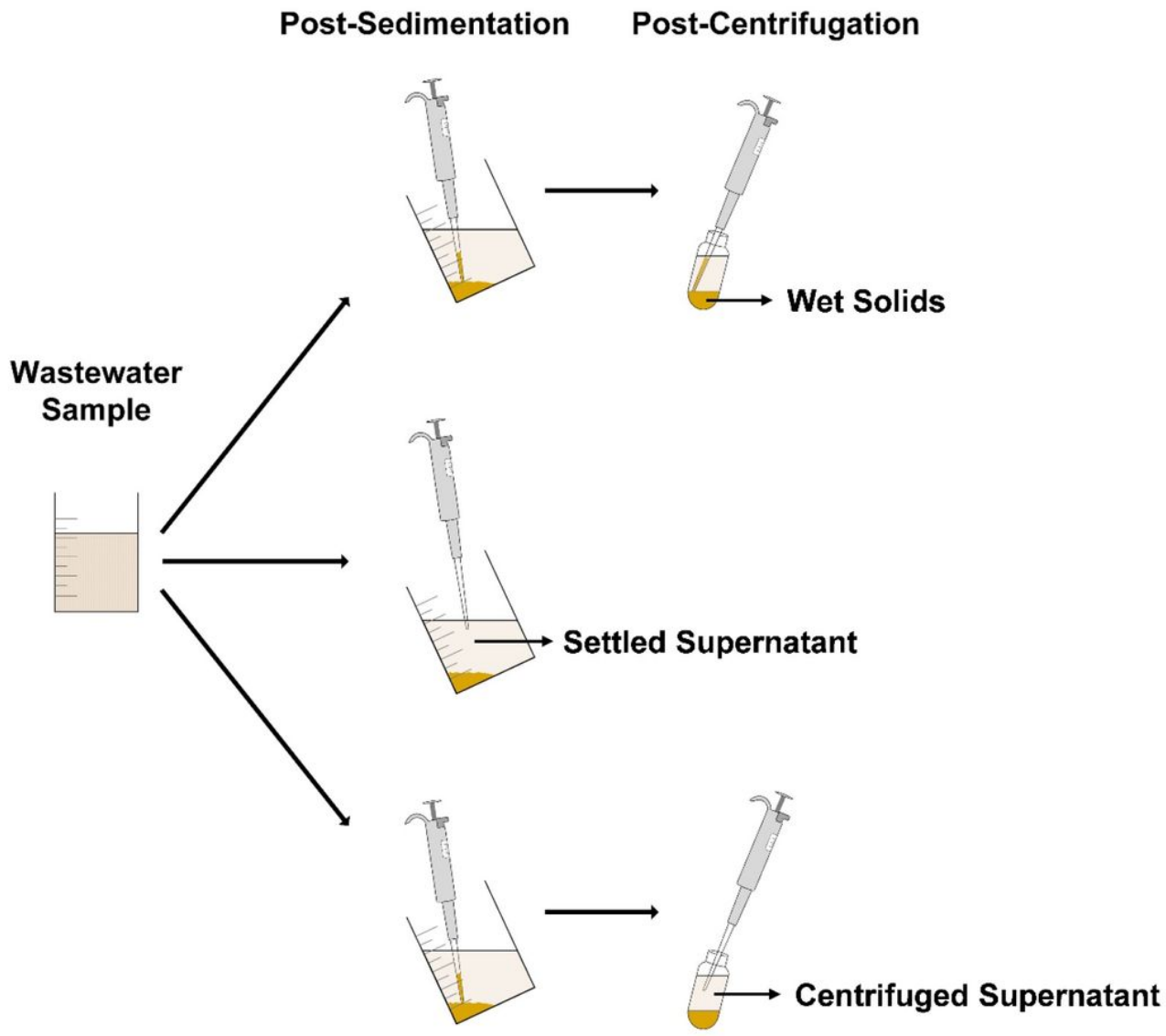

Figure 2

Wastewater sample fractions post-sedimentation and post-centrifugation analyzed in this study

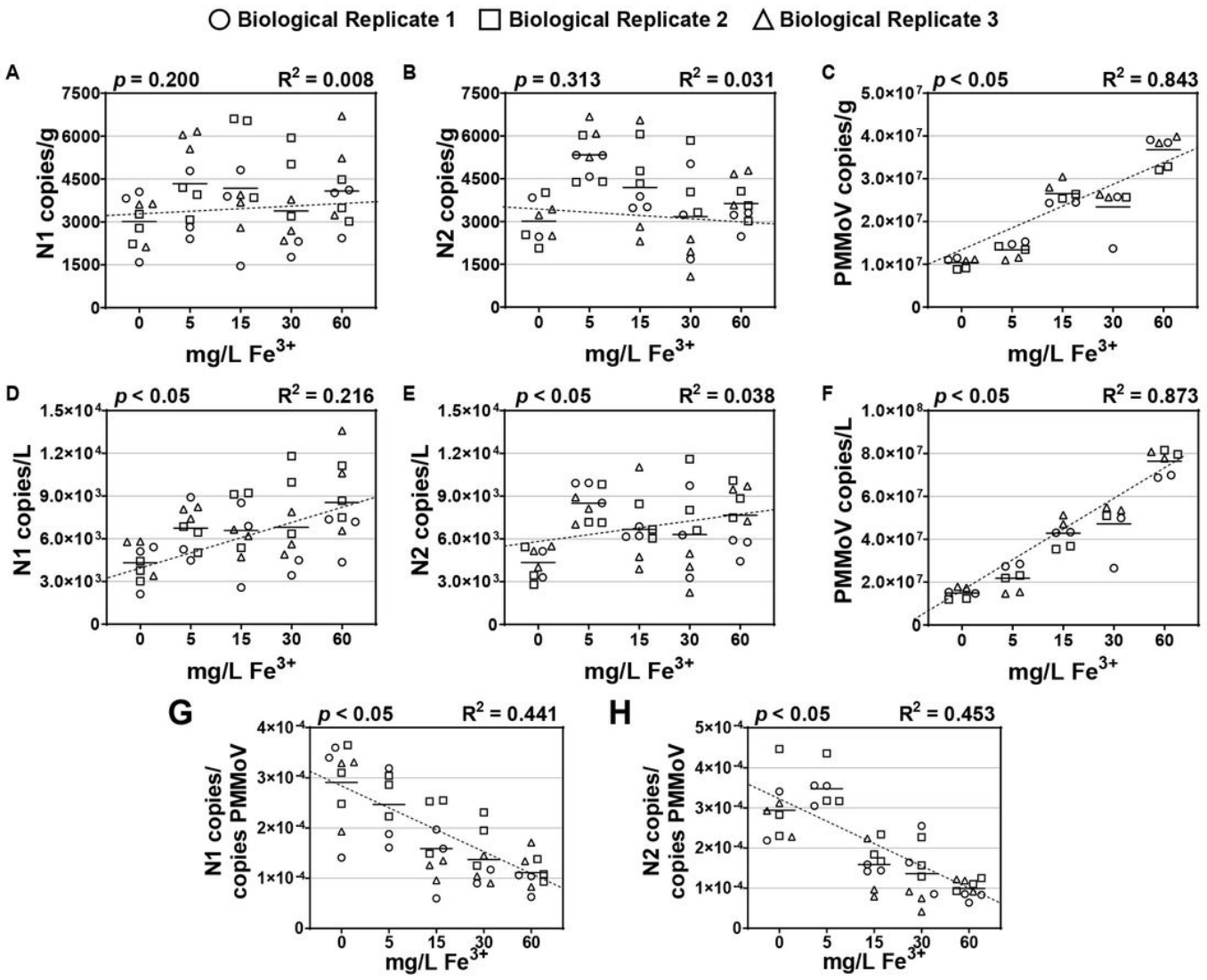

Figure 3

Effect of increasing coagulant concentrations on: (A) N1 copies/g extracted mass, (B) N2 copies/g extracted mass, (C) PMMoV copies/g of extracted mass, (D) N1 copies/L of total sample volume, (E) N2 copies/L of total sample volume, (F) PMMoV copies/L total sample volume, (G) N1 copies/copies PMMoV, and (H) N2 copies/copies PMMoV.

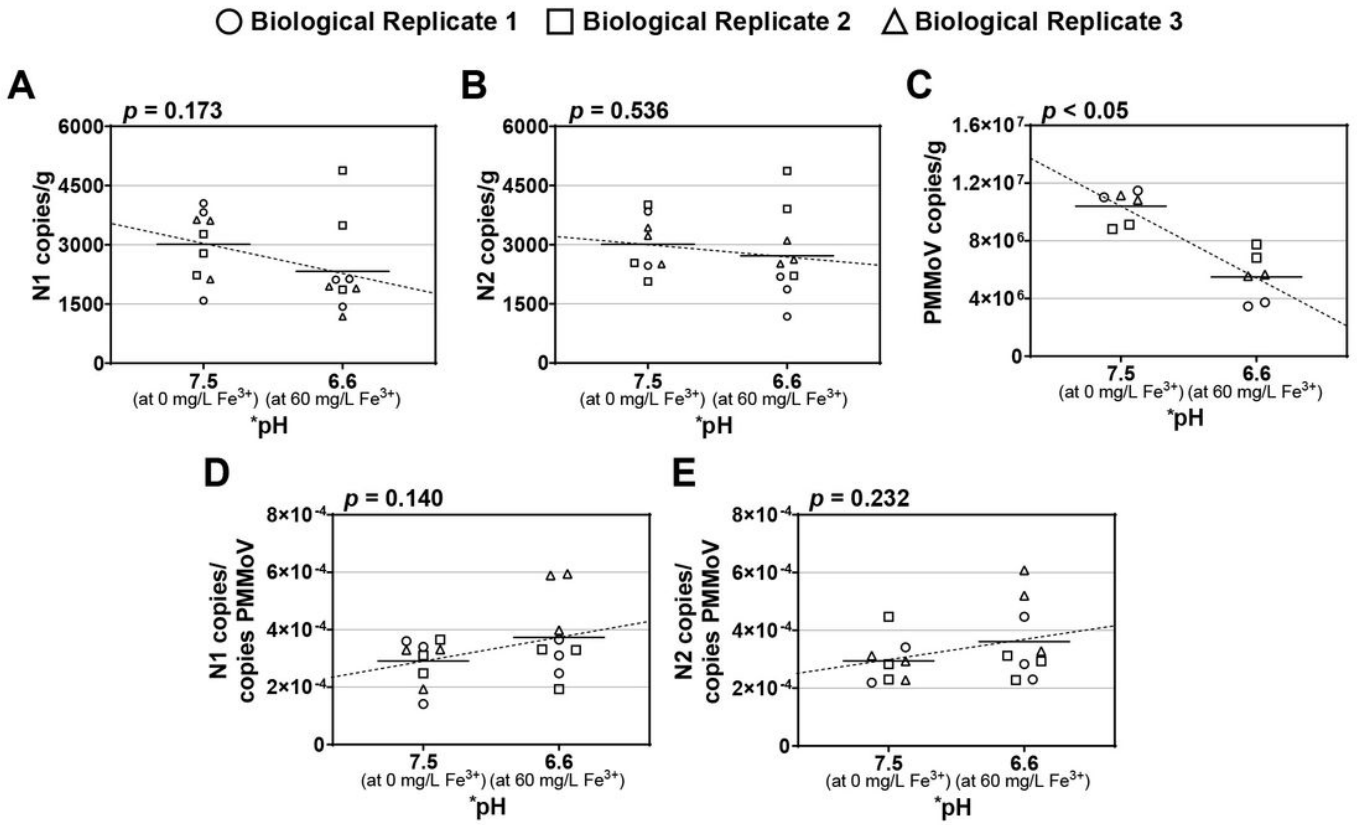

** pH on the x-axis is shown to be decreasing to corresponding to the increasing Fe^{3+} concentrations.*

Figure 4

Effect of pH change on (A) N1 copies/g of extracted mass, (B) N2 copies/g of extracted mass, (C) PMMoV copies/g of extracted mass, (D) N1 copies/copies PMMoV, and (E) N2 copies/copies PMMoV.

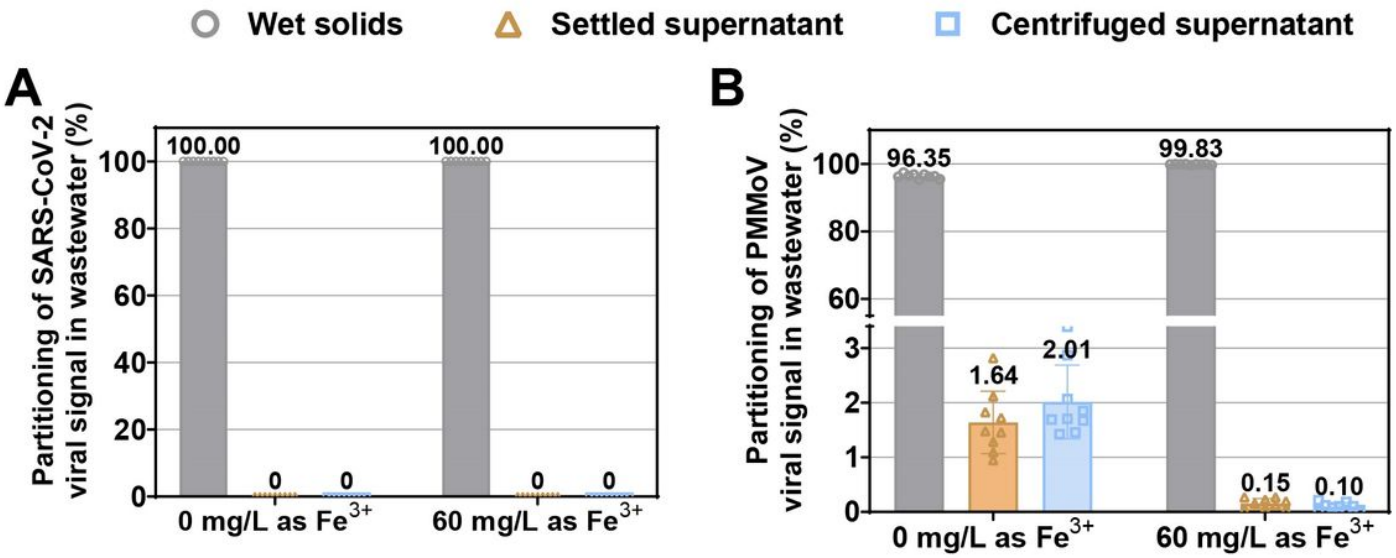

Figure 5

Comparison of the partitioning of (A) SARS-CoV-2 and (B) PMMoV genomic copies. The bars represent the standard deviation (SD) of each measurement and the number on top of each bar is the mean percentage for the measurements.

Supplementary Files

This is a list of supplementary files associated with this preprint. Click to download.

- Hegazyetal.2023Supplementalmaterial.docx